Chemoattractant-induced phosphatidylinositol 3,4,5-trisphosphate accumulation is spatially amplified and adapts, independent of the actin cytoskeleton

Chris Janetopoulos*, Lan Ma†, Peter N. Devreotes*, and Pablo A. Iglesias†‡

*Department of Cell Biology, Johns Hopkins University School of Medicine, 725 North Wolfe Street, Baltimore, MD 21205; and †Department of Electrical and Computer Engineering, Johns Hopkins University, 3400 North Charles Street, Baltimore, MD 21218

Edited by Kai Simons, Max Planck Institute of Molecular Cell Biology and Genetics, Dresden, Germany, and approved April 25, 2004 (received for review March 26, 2004)

Experiments in amoebae and neutrophils have shown that local accumulations of phosphatidylinositol 3,4,5-trisphosphate [PI(3,4,5)P_3] mediate the ability of cells to migrate during gradient sensing. To define the nature of this response, we subjected *Dictyostelium discoideum* cells to measurable temporal and spatial chemotactic inputs and analyzed the accumulation of PI(3,4,5)P_3 on the membrane, as well as the recruitment of the enzymes phosphoinositide 3-kinase and PTEN. In latrunculin-treated cells, spatial gradients elicited a PI(3,4,5)P_3 response only on the front portion of the cell where the response increased more steeply than the gradient and did not depend on its absolute concentration. Phosphoinositide 3-kinase bound to the membrane only at the front, although it was less sharply localized than PI(3,4,5)P_3. Membrane-bound PTEN was highest at the rear and varied inversely with receptor occupancy. The localization of PI(3,4,5)P_3 was enhanced further in untreated polarized cells containing an intact cytoskeleton. Interestingly, the treated cells could respond to two independent gradients simultaneously, demonstrating that a response at the front does not necessarily inhibit the back. Combinations of temporal and spatial stimuli provided evidence of an inhibitory process and showed that a gradient generates a persistent steady-state response independent of a previous history of exposure to chemoattractant. These results support a local excitation/global inhibition model and argue against other schemes proposed to explain directional sensing.

Cells are able to sense and migrate along shallow gradients of chemoattractants (1–3). This fascinating process, called chemotaxis, brings leukocytes to sites of infection and allows their trafficking in the immune system, directs cells to the proper locations during embryogenesis, and guides cells in wound healing (4, 5). Chemotaxis also contributes to pathological states such as allergic inflammation and tumor metastasis (6, 7). To sense gradients, cells compare differences in receptor occupancy along their length and convert this signal into a localized response. Research in *Dictyostelium* and neutrophils has shown that upstream signaling components, such as the receptors and G protein subunits, are essentially uniform along the membrane, and biochemical reactions like chemoattractant binding and G protein activation mirror receptor occupancy (8–11). However, a key intermediate in the pathway, phosphatidylinositol 3,4,5-trisphosphate [PI(3,4,5)P_3], is sharply localized at the leading edge of cells exposed to a gradient. This internal spatial sensing mechanism is functional even when cells are immobile and lack an intact cytoskeleton (12, 13). In *Dictyostelium*, PI(3,4,5)P_3 is regulated through recruitment of phosphoinositide 3-kinase (PI3K) and PTEN to the membrane at the "front" and "rear" of the cell, respectively (14, 15). These movements are determined by upstream events and do not depend on the activities of the enzymes.

Although there is general agreement that the shallow gradient must be amplified internally, there are questions about the overall amount, character, and process of amplification. Is a 3-fold amplification sufficient, or is a 100-fold amplification required to localize pseudopodia to the front of a chemotaxing cell? Do levels of signaling molecules increase linearly along the length of the cell, or is there a threshold point where levels start to increase more steeply? Does all of the amplification take place at a single step, or is the overall amplification a product of a series of events? In this light, it would be interesting to learn whether feedback loops, a common mechanism for achieving amplification, are required. To further understand these mechanisms, we have quantified the distribution of PI(3,4,5)P_3, PI3K, and PTEN under varying chemotactic inputs and in the absence and presence of the actin cytoskeleton. Our studies reveal the features of the response that correspond to "amplification" and elucidate mechanisms of gradient sensing and polarization.

The studies also allow us to evaluate proposed models for gradient sensing. Of these, a large class rely on strong positive feedback loops whereby the response becomes localized by selective amplification of signaling molecules at the front (16, 17). Other similar models link a positive action at the front of the cell to an opposing action at the back. For instance, in the "intermediate depletion" mechanism, highly cooperative binding at the front limits the availability of free signaling molecules at the rear (18). Yet another type of model reasons that the initial contact of the chemoattractant with a cell triggers a rapid inhibitory response that spreads across the cell and prevents the posterior from responding (19). When the gradient is repositioned, there is again a "first hit," and the direction of the response is reset. Finally, a scheme referred to as "local excitation–global inhibition" proposes that directional sensing depends on a balance between a rapid local "excitation" and a slower global "inhibition" process (1, 20–22). This model is discussed in greater detail below.

Materials and Methods

Materials. Cy3-cAMP (23) was used as a chemoattractant. Latrunculin A (Molecular Probes) was used to inhibit actin polymerization.

Cell Culture. *Dictyostelium discoideum* cells were cultured in HL5 medium and developed for 5 h in development buffer (10 mM phosphate buffer/2 mM $MgSO_4$/0.2 mM $CaCl_2$), as described (12). Cell lines used included wild-type AX3 cells expressing PH-GFP (8), PI3K2-GFP (15), and PTEN-GFP (14) and *pten*− cells expressing PH-GFP (14). PH-GFP is the PH domain of the cytosolic regulator of adenylyl cyclase,

This paper was submitted directly (Track II) to the PNAS office.

Abbreviations: PI(3,4,5)P_3, phosphatidylinositol 3,4,5-trisphosphate; PI3K, phosphoinositide 3-kinase; LEGI, local excitation global inhibition.

‡To whom correspondence should be addressed. E-mail: pi@jhu.edu.

CRAC, which has the following specifications for phosphoinositides $PI(3,4,5)P_3 > PI(3,4)P_2 \gg PI(4,5)P_2$, PI(3)P, PI (24).

Assays. For the micropipette assays, a micropipette(s) (Eppendorf microinjection system) filled with 10 μM Cy3-cAMP was positioned and, once steady state was reached, images of sensing cells were recorded. A temporal discharge of Cy3-cAMP was attained by pressing the "clean" button on the microinjection system.

Microscopic Analysis. Images of living cells were observed by using a Zeiss inverted microscope (Axiovert 135TV), captured with a Photometrics CoolSNAP charge-coupled device camera (Roper, Tucson, AZ), and collected by using IP LAB (Scanalytics, Fairfax, VA), as described in ref. 12. Excitation and emission filters used were from Chroma set 86007 (Chroma Technology, Brattleboro, VT), Cells were allowed to adhere in a chamber (Lab-Tek) containing 4 ml of developmental buffer.

Data Analysis. Cell outlines were obtained by using edge detection, cluster removal, and segmentation algorithms from the Image Processing toolbox of MATLAB (Mathworks, Natick, MA). Background subtraction was performed on the measured intensities by using prestimulus values from pixels far away from the cell (Cy3-cAMP) or on the cytosol (PH-GFP, PI3K-GFP, PTEN-GFP). We assumed that 6% of the total PTEN was membrane-bound before stimulation (14). For some of the PI3K measurements, Cy3-cAMP concentrations were based on theoretical prediction by using equation 1 in ref. 25, which agreed with those measured. Least-squares fit lines were computed by using EXCEL (Microsoft).

Results

To simultaneously measure the gradient and the response on living cells, we used Cy3-cAMP as chemoattractant and PH-GFP as a measure of $PI(3,4,5)P_3$. Cy3-cAMP fluorescence values were taken just outside the perimeter of the cell, whereas PH-GFP levels were recorded directly on the membrane (Fig. 1). Application of stimuli with a micropipette in an open system allowed rapid modification of spatial and temporal stimuli by changing the location of the tip or the pressure of chemoattractant released. We carried out experiments for both polarized cells, which have an elongated shape, and a defined anterior and posterior, and round immobile cells treated with latrunculin, an inhibitor of actin polymerization. It was evident in both cases that the gradient of cAMP was shallower than that of PH-GFP (Fig. 1 *A* and *B*). We plotted the input, Cy3-cAMP, against the output, membrane-bound PH-GFP, both normalized by their respective mean values (Fig. 1*C*). These data lead to two major conclusions. First, the output did not mirror the input. If it did, the expected plot would be a line through the origin with a slope of one. Instead, the x-intercept revealed a relative threshold: there was no response where the local cAMP concentration was below the mean level. It is this threshold effect that acts as the primary differentiation between anterior and posterior regions of the cell. Moreover, at concentrations of cAMP that did elicit a response, the curve appeared linear with a slope significantly greater than one. Thus, "amplification" consists of both a threshold and a slope that is greater than one $\{d[PI(3,4,5)P_3]/d[cAMP] > 1\}$. Second, these features were present in both polarized and latrunculin-treated cells, although polarized cells had a slightly higher threshold (0.89 ± 0.11 vs. 0.75 ± 0.13) and a steeper slope (7.1 ± 3.5 vs. 3.1 ± 0.89). This is in contrast to a previous report asserting no amplification of $PI(3,4,5)P_3$ accumulation in latrunculin-treated neutrophils (i.e., the input–output curve would pass through the origin with unit slope) (26, 27). Our observations clearly show significant amplification of $PI(3,4,5)P_3$ in immobilized cells.

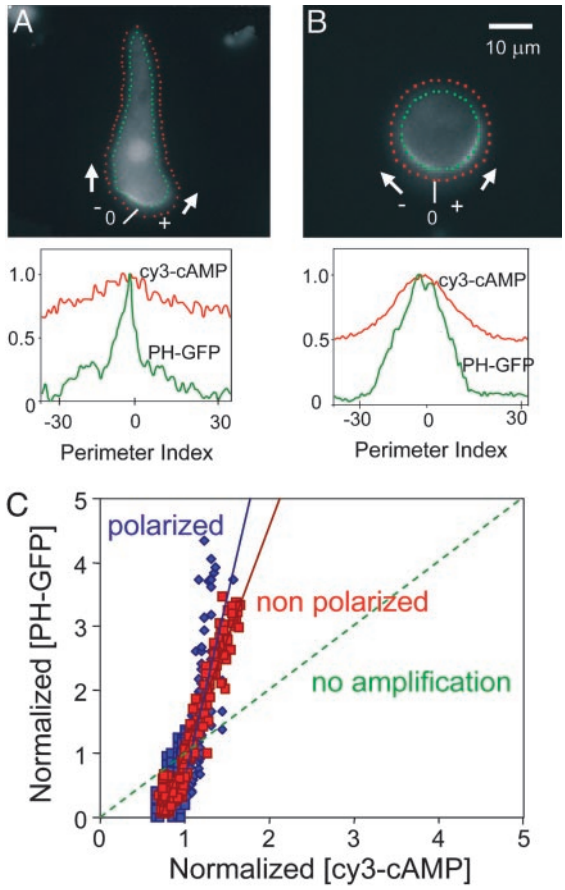

Fig. 1. Measuring the input–output relationship. The spatial distribution of Cy3-cAMP concentration was quantified by measuring fluorescent intensity levels at points just outside the cell perimeter (red dots). Similarly, $PI(3,4,5)P_3$ levels were obtained by measuring the intensity of PH-GFP directly on the cell membrane (green dots) for both polarized (*A*) and latrunculin-treated (*B*) cells. Measured regions contained three adjacent pixels, and their averaged value was plotted. Only representative dots are shown, and at least 64 points were measured for each cell. At each point along the perimeter, where 0 denotes an arbitrary origin, the Cy3-cAMP (red) and PH-GFP (green) concentrations, normalized by their respective maxima, were plotted (*Lower*). (*C*) To quantify the degree of amplification, we plotted the output (PH-GFP concentration, normalized to the mean level for each cell) against the input (Cy3-cAMP concentration, normalized to its mean level). The dotted green line shows the expected plot for a system with no amplification. Data for three polarized cells (blue diamonds) and three latrunculin-treated cells (red squares) are included. Lines are least-squares fit.

We further characterized the responses of immobilized cells when presented with gradients of various slopes (Fig. 2). Cells responded over a wide range of cAMP profiles of varying steepness (from 20% to 300% difference between front and back) and midpoint concentrations (ranging over 2 orders of magnitude). Fig. 2*B* shows the response for the same cell in two different gradients. These demonstrate that the same absolute level of receptor occupancy can elicit vastly different responses depending on whether they occur at the front or rear of the cell. However, input–output relationships, once normalized, produced curves with nearly identical slopes and thresholds (Fig. 2*C*). This means that the intensity of the response depends on the relative steepness of the gradient rather than the absolute concentration of the stimulus. This dependence on gradient steepness has been observed previously for chemotactic responses (28, 29). Our results indicate that $PI(3,4,5)P_3$ may mediate this feature of chemotaxis.

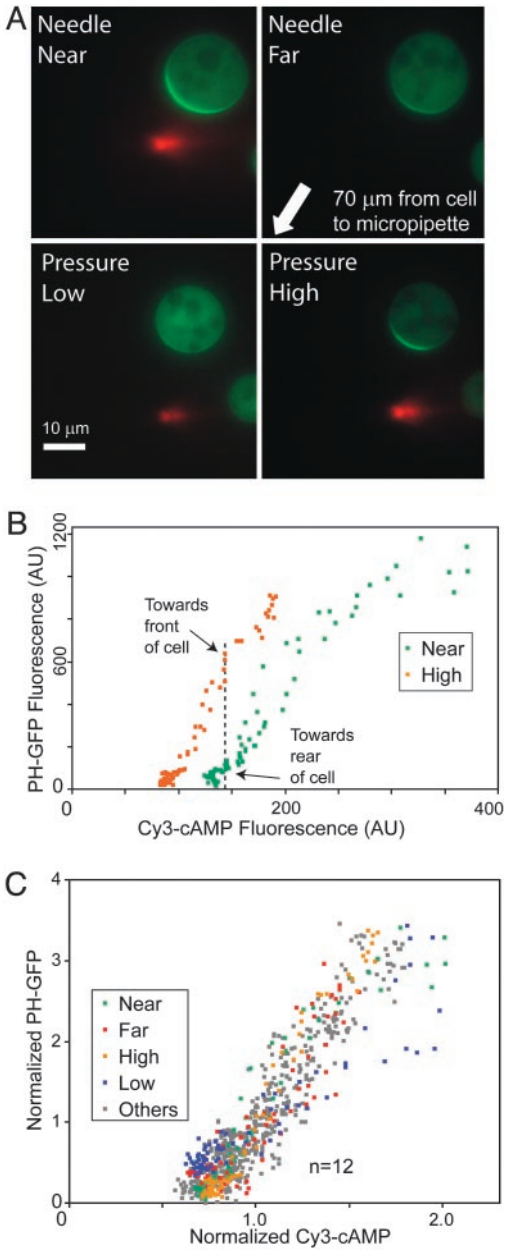

Fig. 2. Response to gradients of varying steepness and absolute concentrations. The input–output response of latrunculin-treated cells under varying chemotactic gradients was quantified as in Fig. 1. The micropipette location and pressure were altered to change the steepness and midpoint of the Cy3-cAMP gradient. Cells were exposed to steep gradients (needle near) and shallow gradients (needle far). The midpoint concentration of chemoattractant was varied by changing the pressure in the micropipette (pressure high and low). (*B*) Shown are the Cy3-cAMP and PH-GFP fluorescence levels for the same cell in two different gradients. Following the dotted line, it is clear that the same Cy3-cAMP concentration elicited vastly different PH-GFP responses. (*C*) Input–output data were normalized and graphed as in Fig. 1*C* for the four examples shown as well as eight other conditions in various cells. Here the responses coincided, showing that the cells' response depends on the relative gradient.

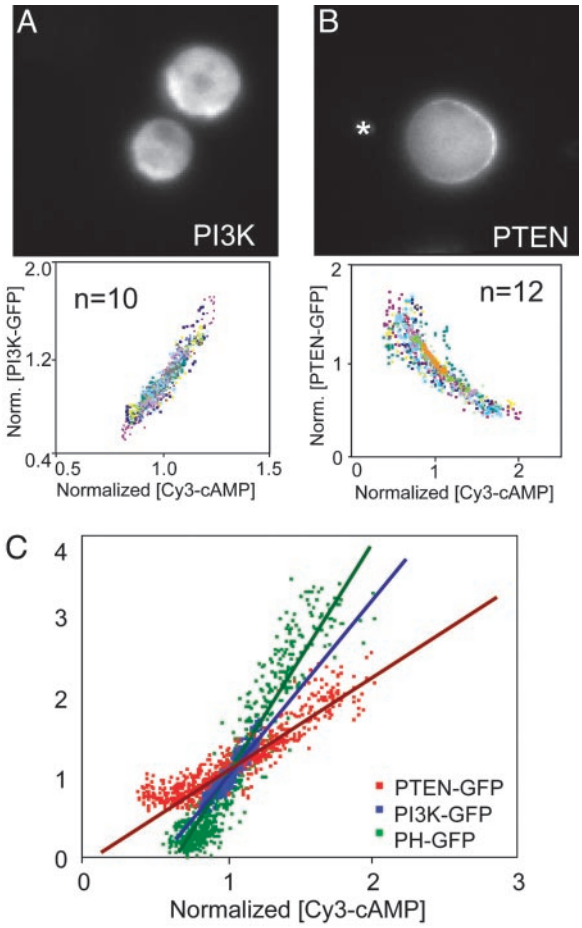

Fig. 3. Response of PI 3′ enzymes. Input–output response of latrunculin-treated cells expressing PI3K-GFP (*A*) or PTEN-GFP (*B*) under varying chemotactic gradients was quantified as in Fig. 1. (*A Upper*) The pipette is located 10 μm below the bottom-left corner of the frame; (*B*) the location is denoted by the asterisk. For both cell types, the individual responses coincided, showing that the enzyme responses also depend on the relative gradient. (*C*) To compare their relative degrees of amplification, we plotted input–output curves for the PI3K, PI(3,4,5)P_3, and the inverse of PTEN. Straight lines are least-squares fits.

To determine the origin of the observed amplification, we characterized the response of the enzymes controlling PI(3,4,5)P_3 levels. Previous results have shown that each of these enzymes must be recruited to the membrane to be active, and for PI3K, activity mirrors localization (24). We imaged simultaneously Cy3-cAMP and either PI3K-GFP or PTEN-GFP in immobilized latrunculin-treated cells (Fig. 3). Like PH-GFP, PI3K-GFP formed a crescent toward the pipette (Fig. 3*A*). Normalized data from multiple cells exposed to gradients of different steepness tightly overlapped (Fig. 3*A*). The input–output curve showed an amplified response (threshold 0.51 ± 0.09, slope of 2.15 ± 0.33). The threshold and slope were smaller than that displayed by the distribution of PH-GFP. As previously reported, PTEN-GFP showed a complementary behavior, forming a crescent away from the higher concentration of Cy3-cAMP (Fig. 3*B*). Again, normalized data for multiple cells overlapped. Because membrane-bound PTEN is inversely correlated with receptor occupancy, we plotted the inverse of PTEN-GFP values (output) against the Cy3-cAMP concentration (input) for convenient comparison with PI(3,4,5)P_3 and PI3K. At the lowest chemoattractant concentration, PTEN values change very little, but the rest of the curve goes through the origin (threshold is 0.08) with a slope of 1.1 (Fig. 3*C*), indicating little amplification. It appears that PI3K provides a significant portion of the PI(3,4,5)P_3 amplification with PTEN contributing an additional component. Together, these distributions account for nearly all of the observed amplification in PI(3,4,5)P_3. In polarized cells, it is apparent that each enzyme displays further localization, most

CELL BIOLOGY

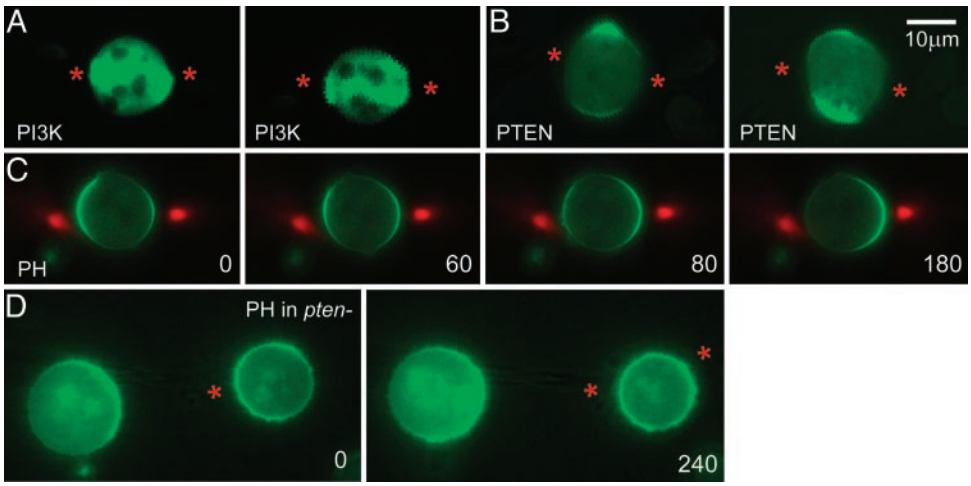

Fig. 4. Response to multiple simultaneous sources. Two micropipettes were brought in close proximity to latrunculin-treated cells creating cAMP profiles with two sharp gradients on either side. (*A*) PI3K-GFP localized to both ends of the cells. (*B*) PTEN-GFP relocalized to the cell membrane at the point of lowest cAMP concentration. (*C*) Cells expressing PH-GFP adjusted to changes in the Cy3-cAMP profile. At time 0 s, the concentration on the left was higher, whereas at 180 s, the profile was reversed. (*D*) *pten*− cells expressing PH-GFP respond to one micropipette at time 0 s. Note the broad crescent response on both cells. A second gradient was applied to the cell on the right at 30 s (not shown). A stable response is shown at 240 s. The cell on the right is incapable of responding with two sharp crescents as in *C*.

likely accounting for the increased amplification in $PI(3,4,5)P_3$ distribution in those cells.

Because most of the amplification occurred in immobilized cells and the responses were very stable, we used the treated cells to assess a variety of stimulus paradigms to distinguish putative sensing mechanisms. Remarkably, when a latrunculin-treated cell was exposed to two very steep gradients from a pair of micropipettes, it responded on both ends (Fig. 4). PI3K and PH domains moved to the poles (Fig. 4 *A* and *C*) and PTEN-GFP moved to the midline (Fig. 4*B*). By carefully adjusting the pressure in each pipette, the $PI(3,4,5)P_3$ signal could be gradually extinguished and restored on either end. In similar experiments,

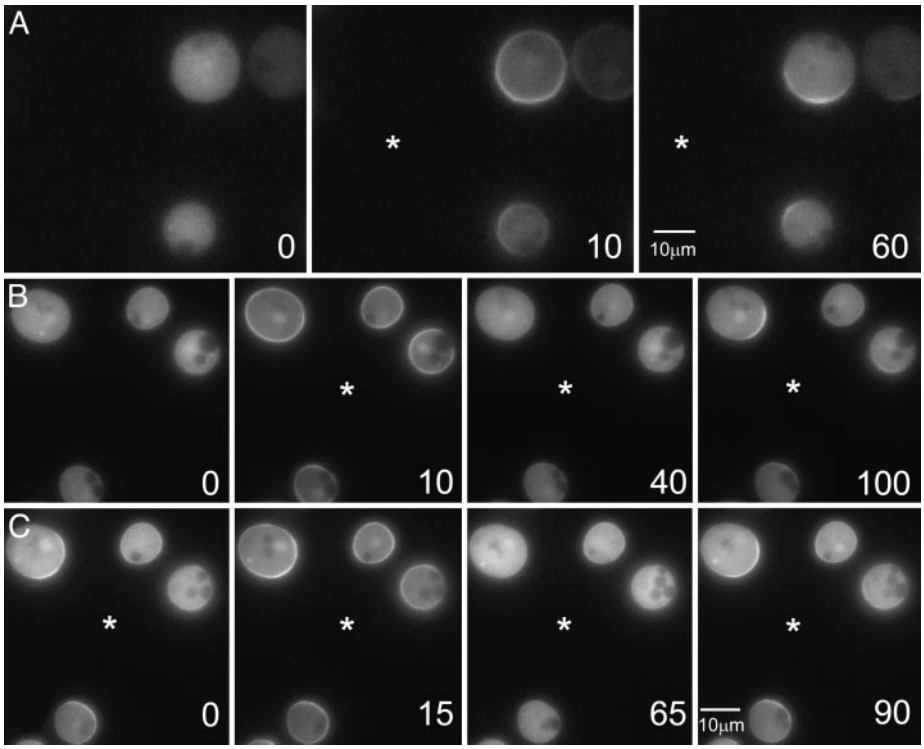

Fig. 5. Response of cells to combinations of stimuli. Cells were exposed to sequential temporal and spatial stimuli, and images were captured. (*A*) A micropipette (location denoted by the asterisk) producing a stable Cy3-cAMP gradient was introduced to naïve cells after the first frame (0 s). (*B*) Naïve cells (0 s) were stimulated by the addition of a micropipette producing a shallow chemoattractant gradient that was immediately pumped to generate a large transient stimulus. Fluorescent images of the Cy3-cAMP used in these experiments demonstrated that the stimulus from the initial bolus dissipated in the 4-ml chamber, and the stable gradient was established within 15 s (data not shown). (*C*) The previous experiment was repeated for cells originally in a gradient (0 s). The micropipette was pumped at 5 s. All results were reproducible (see Movies 1–3).

PTEN-GFP moved in a reciprocal manner. Cells also exhibited two distinct $PI(3,4,5)P_3$ crescents when micropipettes were as little as 90° apart (data not shown). Cells lacking PTEN failed to display two $PI(3,4,5)P_3$ crescents because each response was much broader than that in wild-type cells (Fig. 4*D* and ref. 14). With polarized cells, it was difficult to obtain a stable bipolar response, because the cells tended to choose one micropipette and move toward it (30).

We next exposed the cells to combinations of stimulus increases and gradients to explore the temporal and spatial sensing mechanisms (Fig. 5 and Movies 1–3, which are published as supporting information on the PNAS web site). When a cell was initially exposed to a cAMP gradient, which of course would contain a temporal component, a response ensued along the entire perimeter (Fig. 5*A*). $PI(3,4,5)P_3$ then gradually localized at the side of the cell facing the micropipette. Next, a micropipette was brought in close proximity to cells, immediately discharged to produce a transient bolus of cAMP, which saturated cAMP receptors and then allowed generation of a steady-state gradient at a lower midpoint concentration (Fig. 5*B*). $PI(3,4,5)P_3$ accumulated throughout the membrane in response to the uniform stimulus, then disappeared. $PI(3,4,5)P_3$ then gradually reappeared as a crescent on the side of the cell facing the micropipette as the sensing mechanism reached steady state. Finally, cells initially displaying a $PI(3,4,5)P_3$ crescent were exposed to a transient uniform stimulus (Fig. 5*C*). These cells also responded along their entire perimeter and adjusted to the gradient in the same manner as those in Fig. 5*B*. This sequence shows that the rear of a latrunculin-treated cell remains sensitive to a uniform stimulus and was consistent with the cells' ability to respond to two gradients. In contrast, it was previously reported that the posterior of a polarized cell is relatively insensitive to further stimulation (8).

Discussion

Our quantitative measurements of cAMP, PI3K, PTEN, and $PI(3,4,5)P_3$ to temporal and spatial stimuli have allowed us to characterize the nature of gradient amplification. In a chemoattractant gradient there is a threshold; that is, there is no $PI(3,4,5)P_3$ accumulation on the membrane at the rear of the cell. This is remarkable, because receptor occupancy between front and rear does not differ greatly. Thereafter, the phosphoinositide increases about three to seven times more steeply than receptor occupancy. The $PI(3,4,5)P_3$ distribution is a product of the local activities of PI3K and PTEN. PI3K shows a profile similar to that of $PI(3,4,5)P_3$, although the increase begins closer to the rear and the slope thereafter is lower. In contrast, PTEN binding is inversely correlated with receptor occupancy, with a linear dependence along the entire length of the cell. These data indicate PI3K-induced synthesis does not account for all of the spatial localization of $PI(3,4,5)P_3$. PTEN sharpens this profile by degrading the lipid near the rear. Moreover, because $PI(3,4,5)P_3$ levels resemble the ratio, PI3K/PTEN, this suggests that lipid dispersion does not blur this profile. The more localized profile of PI3K suggests that a different mechanism controls its binding than that of PTEN.

These experiments highlight the differences between gradient sensing and polarization, reviewed in ref. 30. Polarized cells have distinct front and rears defined by the accumulation of specific molecules such as actin and myosin and differences in their sensitivity at the two ends. Latrunculin-treated cells lose polarity and can accumulate PI3K and $PI(3,4,5)P_3$ on both ends and PTEN toward the middle, indicating that they do not have predefined fronts and backs. Rather, a cell can form two fronts and a "back" at the midline reminiscent of a dividing cell. In fact, we have noted that $PI(3,4,5)P_3$ and PTEN accumulate on the poles and midline, respectively, of cells undergoing cytokinesis (unpublished work). In contrast, polarized cells were incapable of stably responding simultaneously at the front and back (8).

The chemosensory system of the cell responds transiently to stimulus increments yet persistently to stable gradients. Our observations indicate that the two types of responses are generated by the same internal mechanism. The transient disappearance of the crescent in Fig. 5*C* after the addition of a uniform stimulus provides strong evidence for a chemoattractant-induced inhibitor that dissipates slowly when the stimulus is removed. This series of experiments also shows that an equivalent gradient will generate the same response whether it is formed by increasing the concentration at the front or by decreasing it at the rear of the cell. In fact, the final steady-state response of the cell is completely independent of the stimulus history of the cell.

The quantitative analysis of spatial and temporal PI3K, PTEN, and $PI(3,4,5)P_3$ accumulations to defined chemotactic stimuli allows comparison of models of gradient sensing. Models that rely on strong autocatalytic positive feedback loops provide large amplification but also result in responses that are relatively independent of the external signal. Thus, they are unable to account for the cells' ability to have graded responses that are proportional to the relative gradient or the capacity to adjust

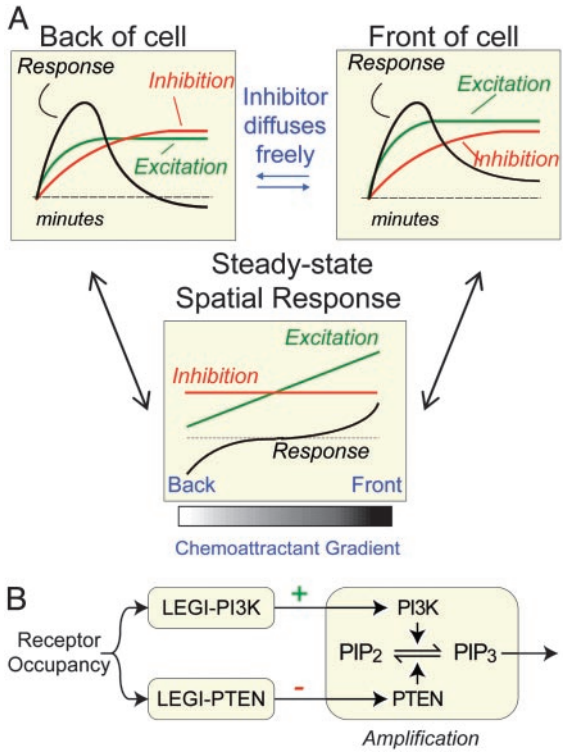

Fig. 6. The LEGI model for gradient sensing. (*A*) Receptor occupancy regulates two opposing processes, excitation and inhibition, which together regulate the response (green, red, and black lines, respectively). When a cell is initially exposed to a gradient, both ends respond. The fast local excitation process increases proportionally to the local fraction of occupied receptors. The slow inhibitory response rises, driven by the global fraction of occupied receptors. When both processes reach a steady state (*Lower*), the profile of excitation along the length of the cell is proportional to the local fraction of receptor occupancy, whereas the global inhibitor is proportional to the mean level of occupied receptors. Thus, at the front of the cell, excitation exceeds inhibition, leading to a persistent response, whereas at the rear, inhibition exceeds excitation, and no positive response is elicited. (*B*) Our data suggest a model in which parallel LEGI mechanisms regulate PI3K and PTEN accumulations on the membrane. Their complementary action sharpens the $PI(3,4,5)P_3$ response.

rapidly to changing stimuli as demonstrated in Figs. 2, 3, and 5 (16–18). The "intermediate depletion" model cannot easily explain the ability of a cell to respond with the same amplification to gradients of varying steepness and midpoint. Similarly, models in which the signaling asymmetry is established by locally deactivating the rear of the cell cannot readily explain the responses to dual stimulation or the ability of a cell to accumulate $PI(3,4,5)P_3$ locally in a gradient after a uniform stimulus (as in Figs. 4 and 5 *B* and *C*) (18, 19). Our data will allow these models to be quantitatively tested and evaluated.

We have previously proposed a model to explain how temporal responses triggered by stimulus increments relate to the spatial responses of cells in gradients (1, 20–22). In the local excitation global inhibition (LEGI) model, spatial sensing involves two opposing processes, a rapid local excitation and a slower global inhibition (Fig. 6*A*). Receptor occupancy controls the steady-state levels of each process, and the balance between the two regulates the response. At the front of the cell, excitation exceeds inhibition because the latter depends on average receptor occupancy. At the back, the situation is reversed. Our data suggest that binding of PI3K and PTEN is regulated by separate LEGI mechanisms, each with its own excitation and inhibition processes (Fig. 6*B*). Because PI3K and PTEN are reciprocally regulated, $PI(3,4,5)P_3$ serves as an amplified readout of this sensing mechanism. We have found that the complementary regulation of the two enzymes gives further amplification at the level of $PI(3,4,5)P_3$ (ref. 31; unpublished work). Based on a mathematical description of this model (21), we have developed an interactive applet that allows a user to visualize the spatial response to various temporal and spatial stimuli in an imaginary cell (32). When exposed to a uniform stimulus, the virtual cell shows a transient response that returns to basal levels with a characteristic time course. When a micropipette is brought in the vicinity of the imaginary cell, the cell responds with a stable crescent. Moreover, the cell is able to form a steady bipolar response when exposed to two micropipettes and shows a greater response toward micropipettes that have a higher concentration (32). Furthermore, the response of the virtual cell to combinations of temporal and spatial stimuli is in qualitative agreement with the observed $PI(3,4,5)P_3$ response.

These findings can now be used to modify mathematical models and account for the observed threshold and gain. Although this LEGI mechanism explains gradient sensing well, it is clear that for polarized cells additional amplification steps are needed. In fact, elements of the other models may be useful to explain the spontaneous polarization and hysteretic behaviors of cells. These features could be effected through actin-dependent positive-feedback loops. Elements of directional sensing and polarization are likely conserved among amoebae, leukocytes, and other cell types. The ability to sense chemical gradients is certainly not restricted only to those cells that respond to chemotactic stimuli but is likely a broad phenomenon that affects many cell types during developmental and tissue differentiation. Moreover, we have not observed a difference in the kinetics of transient $PI(3,4,5)P_3$ accumulation between latrunculin-treated and untreated cells when given a uniform stimulus (data not shown), as would be expected if polymerized actin is involved in a biochemical feedback loop. We find that the differences in gradient amplification between treated and untreated cells (Fig. 1) may represent feedback from the cytoskeleton of a polarized cell on the signaling apparatus (30).

We thank Masahiro Ueda (Osaka University, Osaka) for kindly providing the Cy3-cAMP. This research was supported by National Institutes of Health Grants 34933 and 28007 (to P.N.D.), American Cancer Society Grant PF-00-334-01 (to C.J.), the Whitaker Foundation, and National Science Foundation Grant 083500 (to P.A.I.).

1. Parent, C. A. & Devreotes, P. N. (1999) *Science* **284,** 765–770.
2. Chung, C. Y., Funamoto, S. & Firtel, R. A. (2001) *Trends Biochem. Sci.* **26,** 557–566.
3. Weiner, O. D. (2002) *Curr. Opin. Cell Biol.* **14,** 196–202.
4. Carlos, T. M. (2001) *J. Leukocyte Biol.* **70,** 171–184.
5. Thelen, M. (2001) *Nat. Immunol.* **2,** 129–134.
6. Murphy, P. M. (2001) *N. Engl. J. Med.* **345,** 833–835.
7. Condeelis, J. S., Wyckoff, J. B., Bailly, M., Pestell, R., Lawrence, D., Backer, J. & Segall, J. E. (2001) *Semin. Cancer Biol.* **11,** 119–128.
8. Jin, T., Zhang, N., Long, Y., Parent, C. A. & Devreotes, P. N. (2000) *Science* **287,** 1034–1036.
9. Xiao, Z., Zhang, N., Murphy, D. B. & Devreotes, P. N. (1997) *J. Cell Biol.* **139,** 365–374.
10. Servant, G., Weiner, O. D., Neptune, E. R., Sedat, J. W. & Bourne, H. R. (1999) *Mol. Biol. Cell* **10,** 1163–1178.
11. Janetopoulos, C., Jin, T. & Devreotes, P. (2001) *Science* **291,** 2408–2411.
12. Parent, C. A., Blacklock, B. J., Froehlich, W. M., Murphy, D. B. & Devreotes, P. N. (1998) *Cell* **95,** 81–91.
13. Servant, G., Weiner, O. D., Herzmark, P., Balla, T., Sedat, J. W. & Bourne, H. R. (2000) *Science* **287,** 1037–1040.
14. Iijima, M. & Devreotes, P. (2002) *Cell* **109,** 599–610.
15. Funamoto, S., Meili, R., Lee, S., Parry, L. & Firtel, R. A. (2002) *Cell* **109,** 611–623.
16. Meinhardt, H. (1999) *J. Cell Sci.* **112,** 2867–2874.
17. Narang, A., Subramanian, K. K. & Lauffenburger, D. A. (2001) *Ann. Biomed. Eng.* **29,** 677–691.
18. Postma, M. & Van Haastert, P. J. (2001) *Biophys. J.* **81,** 1314–1323.
19. Rappel, W. J., Thomas, P. J., Levine, H. & Loomis, W. F. (2002) *Biophys. J.* **83,** 1361–1367.
20. Devreotes, P. N. & Zigmond, S. H. (1988) *Annu. Rev. Cell Biol.* **4,** 649–686.
21. Levchenko, A. & Iglesias, P. A. (2002) *Biophys. J.* **82,** 50–63.
22. Iglesias, P. A. & Levchenko, A. (2002) *Sci. STKE*, RE12.
23. Sako, Y., Hibino, K., Miyauchi, T., Myamoto, Y., Ueda, M. & Yanagida, T. (2000) *Single Mol.* **1,** 159–163.
24. Huang, Y. E., Iijima, M., Parent, C. A., Funamoto, S., Firtel, R. A. & Devreotes, P. (2003) *Mol. Biol. Cell* **14,** 1913–1922.
25. Segall, J. E. (1993) *Proc. Natl. Acad. Sci. USA* **90,** 8332–8336.
26. Weiner, O. D., Neilsen, P. O., Prestwich, G. D., Kirschner, M. W., Cantley, L. C. & Bourne, H. R. (2002) *Nat. Cell Biol.* **4,** 509–513.
27. Wang, F., Herzmark, P., Weiner, O. D., Srinivasan, S., Servant, G. & Bourne, H. R. (2002) *Nat. Cell Biol.* **4,** 513–518.
28. Zigmond, S. H. (1977) *J. Cell Biol.* **75,** 606–616.
29. Fisher, P. R., Merkl, R. & Gerisch, G. (1989) *J. Cell Biol.* **108,** 973–984.
30. Devreotes, P. & Janetopoulos, C. (2003) *J. Biol. Chem.* **278,** 20445–20448.
31. Krishnan, J. & Iglesias, P. A. (2004.) *J. Theor. Biol.* **229,** 85–99.
32. Kutscher, B., Devreotes, P. & Iglesias, P. A. (2004) *Sci. STKE*, pl3.